

# A geometric view of quantum cellular automata

Jonathan R. McDonald<sup>a</sup>, Paul M. Alsing<sup>a</sup>, and Howard A. Blair<sup>b</sup>

<sup>a</sup>Air Force Research Laboratory, Information Directorate, Rome, New York 13441;

<sup>b</sup>Department of Computer Science and Electrical Engineering, Syracuse University, Syracuse, New York

## ABSTRACT

Nielsen, *et al.*<sup>1,2</sup> proposed a view of quantum computation where determining optimal algorithms is equivalent to extremizing a geodesic length or cost functional. This view of optimization is highly suggestive of an action principle of the space of  $N$ -qubits interacting via local operations. The cost or action functional is given by the cost of evolution operators on local qubit operations leading to causal dynamics, as in Blute *et. al.*<sup>3</sup> Here we propose a view of information geometry for quantum algorithms where the inherent causal structure determines topology and information distances<sup>4,5</sup> set the local geometry. This naturally leads to geometric characterization of hypersurfaces in a quantum cellular automaton. While in standard quantum circuit representations the connections between individual qubits, i.e. the topology, for hypersurfaces will be dynamic, quantum cellular automata have readily identifiable static hypersurface topologies determined via the quantum update rules. We demonstrate construction of quantum cellular automata geometry and discuss the utility of this approach for tracking entanglement and algorithm optimization.

**Keywords:** Information geometry, quantum cellular automata, quantum information, quantum computation

## 1. INTRODUCTION

When Richard Feynman<sup>6</sup> introduced the conceptual foundations of quantum computation it was an attempt to ask the question, “What dynamical rules must a computational device admit to efficiently—and *exactly*—simulate Nature?” Feynman only requires physical processing of information through *local* interaction, *one* of the primary features of cellular automata. In this manuscript we follow this lead and want to look at a local geometric view of computation that represents the causal and information dynamics involved in the computation. While we develop a generic approach for quantum computation, we will apply it directly to cellular automata. Cellular automata are particularly interesting given their inherently local behavior and the homogeneity in space and time. As a result the connectedness of the qubits is static and defines a clear notion of how one qubit can effect any other qubit in the system.

A goal of computation is to take a system of qubits in some initial configuration and output a configuration from which we can ascertain the answer to some question of interest. Feynman’s goal was to have a computation that could effectively simulate a quantum system, but we can ask more general questions. In quantum computation, this reduces to accurately and efficiently simulating the action of some arbitrary, but known, unitary operator. One can then ask, given a unitary operator acting on  $N$  qubits, what is the optimal decomposition into local 1, 2, or higher-order qubit interactions? One approach to this was introduced by Nielsen *et. al.*<sup>1,2</sup> using the language of differential geometry in which the optimal algorithm is obtained via the minimal geodesic—according to the inherent Riemannian metric—to the desired unitary. While this approach is reminiscent of an action principle which can be extremized and equations of motion extracted, it is somewhat at odds with typical physical models with actions which are usually aimed at describing some trajectory through configuration space of the physical system, i.e. the qubits. Indeed the geodesics in the space of operators are dual to trajectories of the qubits in configuration space. It is this latter trajectory we hold as a focus for determining the efficient simulation of a given unitary operator.

---

Further author information: (Send correspondence to J.R.M.)

J.R.M.: jmcndld@gmail.com

P.M.A.: paul.alsing@rl.af.mil

H.A.B.: blair@ecs.syr.edu

The beauty of the minimal geodesic interpretation is in its geometric in origin. However, the geodesic approach's natural arena is the space of operators. It is reasonable to think, then, that there exists a dual approach on the configuration of qubits in the computation. In this manuscript we developed a view of computation as an evolution of a geometry of qubits and examine the case of QCA. In Section 2 we will present the foundations relevant to construction of surface geometries of qubits in a computation, including topology construction and metric information. Then in Section 3 we examine QCA as a initial test and toy model of this approach in 1D QCA. We end with a discussion of conclusions from the QCA simulations and future directions.

## 2. FOUNDATIONS: WHAT IS THE GEOMETRY OF A SYSTEM OF QUBITS?

Given a computation that specifies a set of qubits and local interactions. We propose that the content of the computational structure allows for the construction of a low-dimensional manifold ( $\dim(\mathcal{M}) \ll 2^N$ ) for the qubits at any given moment of simultaneity, spatial slice, in the computation. Moreover, the the topological properties of such a manifold represents the connectivity/causal properties of the computation in the future of the given slice. Geometric properties on the topology may be assigned in a number of ways, but a reasonable requirement seems to be that distances should correspond to the informational correlation of local states in the computation, independent of that actual distribution in Hilbert space. Once we have prescription for the computational geometric state, we can construct the geometric evolution of the computation from foliations of the evolution.

We examine in this section the key ingredients to computational manifold construction. A topology tells us which qubits are localized near other qubits in the computation. This is a property of the computation itself encoded in the interconnectivity of the local quantum operations. We interpret each qubit as a point in our topology. What is the topology on the set of qubits? It is true that there is the natural topology on the composite Hilbert space, but such a topology is not necessarily characteristic of the computation and does not provide any simplification over the  $2^N$ -dimensional Hilbert space. Instead the topology of our computational geometry is to be derived from the causal history of qubits in the computation.

Given a topology, the geometric content is contained in the metric information of the (pseudo)-Riemannian manifold. In the computational manifold, metric information corresponds to local distances between neighboring neighborhoods of qubits (or between "nearby" qubits). Such a distance represents the degree to which information contained in two distinct neighborhoods is correlated. Such a measure based on correlated information allows one to use geometric content as a probe of classical and quantum correlations.<sup>5</sup> Below we review the information distance on quantum states and describe a methodology for topology construction on which to assign geometric content.

### 2.1 Information Distance

We have already outlined the broad proposal being investigated, now we must generate the necessary mathematical framework to assign a manifold to an instance in the computation. Given the topology, the closeness of two neighboring qubits is determined by the metric information. Two neighboring qubits neighbor one another if information flow from one qubit to another need not flow through intermediary qubits. However, the topological relation gives no content on the relative distance between any two such topologically nearby qubits. One way to assign quantitative geometric meaning to two information carrying systems is through correlation information. Two qubits can be said to be close if they are strongly correlated and far if they are uncorrelated. One measure of the correlation between two information carrying systems is Zurek's information metric<sup>4</sup>

$$\begin{aligned} \delta(A, B) &= H(A|B) + H(B|A) \\ &= H(AB) - H(A : B) \\ &= 2H(AB) - H(A) - H(B) \end{aligned} \tag{1}$$

where  $H(A)$  is the Shannon entropy on system  $A$ ,  $H(AB)$  is the joint information,  $H(A|B)$  is the conditional information, and  $H(A : B) = H(A) + H(B) - H(AB)$  is the mutual information. On classical systems, this distance satisfies all the criteria for a distance measure to be a metric. The utility of this measure is that it utilizes the joint and local states to provide a true measure of the correlated content of the two subsystems. We

know of no other distance measure that identifies the correlation content between two subsystems of a composite system in a known state. The Zurek information distance is the measure that gives a direct indication of the information overlap between  $A$  and  $B$ , given the joint state of  $AB$ . This is evident from the second line of (1) which captures the essence of information distance (see Figure 1);

$$\left( \begin{array}{c} \text{Information} \\ \text{Distance} \end{array} \right) = \left( \begin{array}{c} \text{Information content of} \\ \text{the joint system, } AB \end{array} \right) - \left( \begin{array}{c} \text{Information common} \\ \text{to both } A \text{ \& } B \end{array} \right) \quad (2)$$

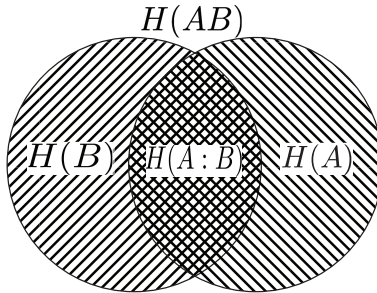


Figure 1. The relationship between marginal, joint and mutual information.

Extension from the classical information metric with Shannon entropy to the quantum, using von Neumann entropy, is not automatic. In the above, the information distance relies the mutual information or the conditional information in two of the classically equivalent formulations. Since conditional information on quantum states presumes some basis of measurement variation of which may generate distinct conditional information outcomes, there must be some care in the information distance as applied to quantum states. The discord,<sup>7</sup> Zurek’s measure of the quantumness of a state, is typically defined as the difference between classically equivalent measures of mutual information. However, the essence of these differences between two such measures applied to quantum states is in the violation of Bayes’ theorem,  $S(A|B) \neq S(AB) - S(B)$ , and the quantum disparity between classically equivalent measures of conditional information. Therefore, if we focus on the conceptual meaning of the information distance as laid out in (2), then we can avoid any problems arising from quantum discord. If we take as the fundamental measure  $\delta(A, B) = 2S(AB) - S(A) - S(B)$ , then we avoid such problems completely.

Another peculiarity, though essential for our purposes, arises with the use of the  $\delta$  information distance. When applied to pure quantum states, the information distance yields 0 for any separable state and a negative distance in the presence of any non-local correlations (Figure 2). When applied to measurement outcomes on singlet states, it is known that this measure fails to satisfy the necessary properties of a (Riemannian) metric.<sup>5</sup> On general quantum states (without conditioning on measurements), the distance satisfies all properties of the metric except in relation to positive-definiteness and the triangle inequalities. However, if we instead think of the information distance as a measure on a pseudo-Riemannian space we can recover the notion of a metric. First, we consider the case of pure, separable states as genuine zero distance. This is reasonable since there exists some basis (unique to each party) such that the probability distribution of measurement outcomes will be identical for the two systems. On the space of 2-qubit density matrices there still exists a distinct set of null distances. It is easily seen from the definition that a composite system will generate null distance between two of its constituent parts when  $S(AB) = S(A) = S(B)$ . Hence, we have a break down into positive distances,  $S(AB) > \frac{1}{2}[S(A) + S(B)]$ , negative distances,  $S(AB) < \frac{1}{2}[S(A) + S(B)]$ , and null distances. Figure 2 shows the information distance as applied to the Werner state. We see the explicit crossing of the null surface long before the system becomes separable but as the classical uncertainty in the joint system play a more important role than the quantum, non-local correlations. It is not clear at this point the meaning of such a situation; however, there are indications that one may be able to distinguish between the classical and quantum correlations through the mutual information.<sup>8</sup> These issues aside, the information distance assigns a metric on a topological scaffolding for our computation. We need only be wary of assigning a particular importance to positive distances. However, negative information distances provide a clear marker for non-local correlations in the system.

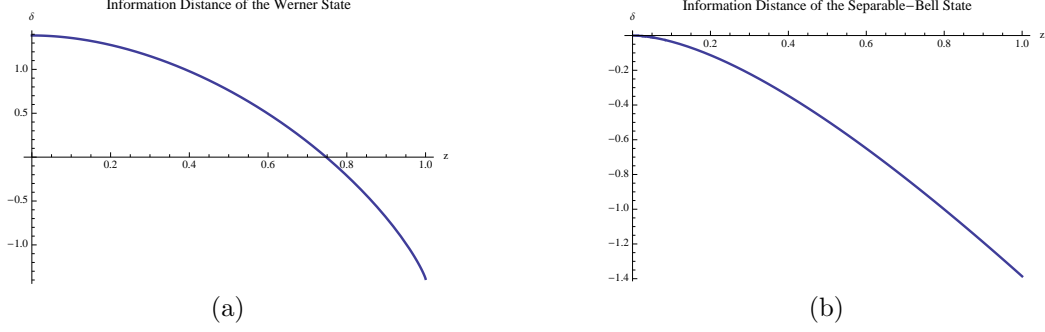


Figure 2. Information distance with classical and quantum correlations: (a) Here we show the mixture of the maximally mixed state with the Bell state  $|\beta_+\rangle = (\sqrt{2})^{-1}(|00\rangle + |11\rangle)$ . The  $z = 0$  axis corresponds to the maximally mixed state while  $z = 1$  corresponds to the pure Bell state. As we can see, the classical correlations quickly overwhelm nonlocal quantum correlations in the information distance. (b) Here we plot the information distance for the state  $|\psi\rangle = \sqrt{1-z}|00\rangle + \sqrt{z}(|01\rangle + |10\rangle)$ . Only for the separable state is the information distance 0, as can be checked with the Peres-Horodecki criterion. For the state with nonlocal quantum correlations, the distance is always negative.

## 2.2 Causal Foliations of Computations

We now shift our focus to construction of the scaffolding on which the above information metric is to be applied. We first review how one constructs foliations, a one-parameter family of non-causally correlated surfaces, of a quantum computation. For any quantum computation there exists a partial order (or causal order) on the unitary operators defining the dynamics given by the ordering of the application of the operators to the qubits. A partially ordered set (poset) is a set of elements endowed with an order  $x \preceq y$ , denoting  $x$  precedes  $y$ , with the following properties;

$$x \preceq x \tag{3a}$$

$$x \preceq y \ \& \ y \preceq x \Rightarrow x = y \tag{3b}$$

$$x \preceq y \ \& \ y \preceq z \Rightarrow x \preceq z. \tag{3c}$$

For two unitaries  $U_i$  and  $U_j$  in a quantum dynamical system, we can say that  $U_i \preceq U_j$  if the commutator  $[U_i, U_j]$  is nonzero and  $U_i$  causally precedes  $U_j$ . This partial order on operators imposes a dual partial order on the Hilbert spaces between successive unitary operators<sup>3</sup> (Figure 3). From here will focus on the poset of Hilbert spaces. The poset on unitaries will play a central role shortly when we construct topologies on slices of a foliation.

The poset encodes the dynamical history of the computation. The content of the poset generates enough information to determine a foliation, and all foliations, of the computation. Similar to general relativity with its natural causal order, there will, in general, be many foliations of the poset. For the purposes here we need only consider one such foliation. Different foliations of the same computation are equivalent under suitable local evolution. We first require a notion of a single surface in the foliation.

**DEFINITION 1.** *An anti-chain,  $A$ , in the poset is a subset such that no two elements are related through the partial order;*

$$A = \{x, y | x \neq y \Rightarrow \text{neither } x \preceq y \text{ nor } y \preceq x\}.$$

*A maximal anti-chain,  $\tilde{A}$ , is an anti-chain such that all elements not in  $\tilde{A}$  are related through the partial order to at least one element in  $\tilde{A}$ .*

A maximal anti-chain of Hilbert spaces forms a global Hilbert space of the computation characterizing a given state of the computation. A computation can then be decomposed into a set of maximal anti-chains:

**DEFINITION 2.** *A foliation on a poset is a collection of maximal anti-chains  $\mathcal{F} = \{\tilde{A}_i\}$  such that  $\tilde{A}_i \cap \tilde{A}_j = \emptyset$  for all  $\tilde{A}_i, \tilde{A}_j \in \mathcal{F}$ .*

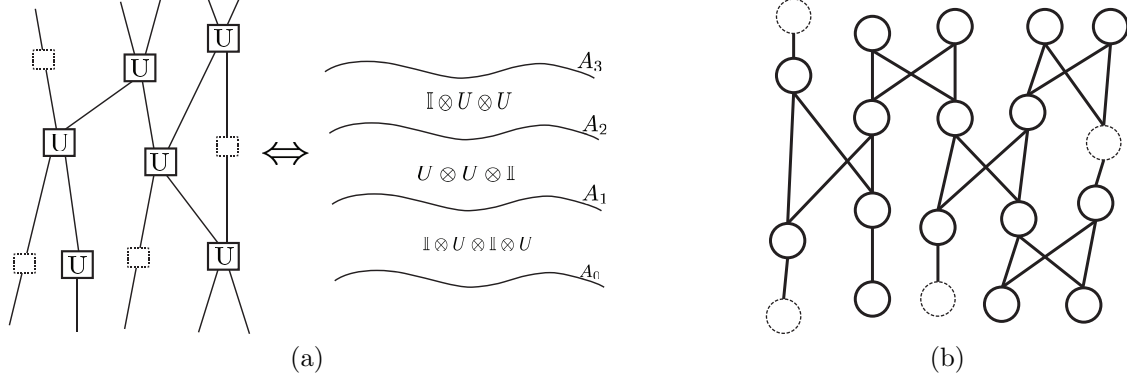


Figure 3. (a) The computation induces an inherent partial order on the local unitaries (boxes) used to decompose a given global operator. Hilbert spaces (wires) connected by two unitaries indicate the partial ordering relation. This partial order induces foliations on the computation. Identity operators (dashed boxes) can be introduced as needed in order to construct non-degenerate surfaces in the foliation. (b) The partial order on the unitaries induces a partial order (lines) on the Hilbert spaces (circles). Whenever an identity operator is introduced, a copy of the Hilbert space (dashed circle) is made and an ordering relation is introduced.

Blute *et. al.*<sup>3</sup> define the process of forming foliations using *locative* slices, which will not generally be maximal anti-chains. We follow a similar procedure in which maximal anti-chains play the pivotal role and may be thought of as complete spatial hypersurfaces/slices of the computation. These surfaces form the global, computational Hilbert space and a state assigned to such a surface is the global state of the  $N$  qubits. Since we only examine maximal anti-chains we will implicitly assume  $A_i = \tilde{A}_i$  for notational simplicity. Assume a maximal anti-chain,  $A_0$ , on the Hilbert spaces, which we will refer to as the initial value data. Generally this set will be taken to be the minimal set with respect to the partial order.  $A_0$  is the input to a set of unitary operators in the computation. Whenever necessary one can split a Hilbert space,  $\mathcal{H}_i$ , into two Hilbert spaces,  $\mathcal{H}_{i_1}$  and  $\mathcal{H}_{i_2}$  such that  $\mathcal{H}_{i_1} \preceq \mathcal{H}_{i_2}$ , with the identity as the operator relating the two spaces. In this case, every state in a Hilbert space on slice  $i$  is causally determined by unitary operators acting on states from slice  $i - 1$ . It is clear that the need for the introduction of identity operators arises from the definition of a foliation in which no two slices can overlap. Without introduction of these trivial mappings, two such slices may be degenerate on a given qubit.

From the global system, we obtain local density matrices through the partial trace;

$$\rho_{i_1 \dots i_n} = \text{Tr}^{j_1 \dots j_m} \rho_{i_1 \dots i_n j_1 \dots j_m}. \quad (4)$$

Since we have implicitly assumed only unitary operators are those allowed in construction of the foliations, we have not needed to distinguish the case where the outcomes of measurements may influence the state. However, it is worth noting that for quantum dynamics where measurements are necessary, one must take care with (4). In particular, it is necessary to ensure that knowledge of outcomes for a measurement that is not causally ordered with respect to a Hilbert space cannot affect a state in that Hilbert space.<sup>3</sup> For the present work with unitary operators, this is not a concern and the above reduction via partial trace is sufficient.

### 2.3 From Foliation to Dynamical Geometries of Qubits

Defining foliation information is insufficient content for assigning geometric information of the kind we seek. Instead, we have to construct the scaffolding onto which distance information will rest. To each slice of a foliation we must be able to assign a corresponding topology. It is known that complete causal information can determine the topology of a causal manifold<sup>9</sup> and this has been proposed as a way to measure topology of space-like hypersurfaces in causal set theory.<sup>10</sup> The tools used here are akin to an expanding field of computational homology<sup>11</sup> and persistent homology.<sup>12,13</sup> We will outline some of the basic ideas and apply them directly to the computational foliation.

We follow Major *et. al.*<sup>10</sup> in our initial construction of the topology for an anti-chain. Implicit in this scheme we will make the assumption that local operations act on finitely many qubits in the system. This is natural for

our construction since it implies that a given local state a qubit only depends on a finite number of interactions with finitely many qubits in the past. We will then modify the approach as necessary to obtain an appropriate simplicial complex on which to assign a metric. Start with a maximal anti-chain,  $A_j$ , on which we desire to prescribe a topology. We first make remarks on notation. We denote the set of points causally influenced by  $x$  as  $\mathcal{J}^+(x) = \{y|y \preceq x\}$ . The set of points causally influencing  $x$  is given by  $\mathcal{J}^-(x) = \{y|x \preceq y\}$ . Because we have included reflexivity,  $x \preceq x$ , in our partial order  $\mathcal{J}^+(x) \cap \mathcal{J}^-(x) = \{x\}$ . A thickened anti-chain  $A_j^i$  of thickness  $i$  is the set

$$A_j^i = \{p \mid \text{card}(\mathcal{J}^-(p) \cap \mathcal{J}^+(A_j)) \leq i + 1 \in \mathbb{N}\} \quad (5)$$

Our assumption earlier that the local unitaries in our computation acts only on finitely many qubits is necessary to ensure that we obtain thickened anti-chains for  $0 < i < \infty$ . Moreover, the set  $A_j^i$  forms a subposet of the global poset. Assume we take a given  $i < \infty$ ; there is a set of maximal elements,  $M_j^i \subset A_j^i$ , since the thickened anti-chain is of finite thickness, i.e. there are finitely many points in the future of any point in  $A_j$ . For any  $m_k \in M_j^i$ , we define the set  $P(m_k, A_j) := P_k = \mathcal{J}^-(m_k) \cap \mathcal{J}^+(A_j)$ . The shadow, or projection, of the causal past of  $m_k$  onto  $A_j$  is given by  $\bar{A}_k = P_k \cap A_j$ . A simplicial complex on  $A_j$  is generated by the following rules: (1) each  $\bar{A}_k$  is assigned a vertex  $v_k$  and (2) any non-empty union of  $(n + 1)$  of the  $\bar{A}_k$  is assigned a  $n$ -simplex. The homology can then be computed on each of these simplicial complexes. Each thickened anti-chain generates a simplicial complex. We look for stable topological properties as identifiers of the topology of  $A_j$  over the set of simplicial complexes generated by increasing the thickness of the anti-chain. For a connected computation, i.e. one where information can transfer information from one segment of the computation to any other, we first allow the manifold to become connected prior to examining stable homology groups. This may seem arbitrary; however, if the computation never achieves a single connected component we are justified in treating the system as two distinct and separable computations from the beginning. However, any computation with all qubits contributing to the computation will generally become connected through a proper assignment of simplicial complexes.

For a quantum computation, each of these  $\bar{A}_k$  will, in general, be a tensor product of single qubit Hilbert spaces. This provides a simplified topology in which groups of points in the original poset are consolidated into a single, local point in the topology. The points then becomes a tensor product of Hilbert spaces in the computation. Instead, we wish to have points in the topology to represent the individual, irreducible Hilbert spaces so as to examine the connectivity of the computation at a given time for a given thickness.

We generate the simplicial complex on individual Hilbert spaces with a related approach that takes into account the unitary operators acting in the computation. We first supplement the poset of Hilbert spaces with the poset of unitaries. There exists a natural partial order between the elements of the two distinct posets: (1) for every Hilbert space  $\mathcal{H}_i$  which is the domain of a unitary  $U$ , we have the relation  $\mathcal{H}_i \preceq U$ . Take a maximal anti-chain  $A_j$  and (2) for every  $\mathcal{H}_j$ , i.e. each wire, which is in the image of  $U$  we have  $U \preceq \mathcal{H}_j$ . Using the other partial order relations on the two sets gives a partial order on the combined set. The elements of  $A_j$  form the vertices  $v_k$  of the collection of simplicial complexes to be generated. Examine the next foliation  $A_{j+1}$  and the unitary operators acting on local subsets of  $A_j$  to generate local subsets of  $A_{j+1}$ . We therefore can introduce a partial order between unitary operators and Hilbert spaces. Recall the construction of the thickened anti-chain, which is the set of points (unitaries for our purposes) in the poset meeting the ‘thickening’ criteria (5). The Hilbert spaces immediately following the maximal unitaries in the thickened anti-chain can be thought of as output Hilbert spaces of a composite unitary whose domain is the anti-chain  $A_j$ . The shadow of a given unitary are thus the Hilbert spaces acting as the domain of the unitary.

A simplicial complex is constructed from the set  $\bar{A}_j(U_i)$  as the shadow of the unitaries  $U_i$  on the anti-chain  $A_j$ ;

$$\bar{A}_j(U_i) = \{x \in \mathcal{J}^-(U_i) \cap A_j\}. \quad (6)$$

To each  $\bar{A}_j(U_i)$  we assign a complete graph or  $k$ -simplex, with  $k+1 = \text{card}[\bar{A}_j(U_i)]$ . For any two  $\bar{A}_j(U_i), \bar{A}_j(U_m)$  with non-empty intersection, there is a simplex connecting them such that the two complete graphs share the boundary given by the complete graph formed through Hilbert spaces in their intersection. This is guaranteed to be a well-defined simplicial complex,<sup>14</sup> analogous to the above the prescription. This gives us a construction for a simplicial complex in which the connectivity of the single qubit Hilbert spaces is made explicit and is a consequence of the causal properties of the computation.

### 3. QUANTUM CELLULAR AUTOMATA

Our interest now shifts to a particular model of computation: quantum cellular automata (QCA).<sup>15–18</sup> QCA are the natural extension of classical cellular automata to the quantum regime. However, a clear understanding of QCA has not yet developed in sufficient detail to say that there exists a complete theory of QCA. Since our goal in this manuscript is not to extract a particular meaning or property of QCA, we will only need to specify the salient definitions and features common to most known models of QCA in order to model a geometry of the computation. We can specify a particular model of QCA useful for simulation and modeling the geometry.

**DEFINITION 3.** *A QCA is a quadruple  $(\mathcal{R}, \Sigma, \mathcal{N}, \mathcal{U})$  consisting of a register  $\mathcal{R} = \mathbb{Z}^d$ , a finite collection of states  $\Sigma$  for each cell in  $\mathcal{R}$ , a collection of local neighborhoods,  $\mathcal{N}$ , and a transition operator on the local neighborhoods,  $\mathcal{U}$ .*

The register  $\mathcal{R}$  labels the sites/qudits for our QCA and the neighborhood specifies the dependencies of the QCA on some finite collection of sites near an  $x \in \mathcal{R}$ . The update rule acts on the neighborhood of  $x$ ,  $\mathcal{N} \cup \{x\}$  to update the qudit at  $x$ . For a given state of the neighborhood of a site, one operates on the site with a single-qudit operator. The total unitary on the neighborhood is then given by  $U(u_1, u_2, \dots, u_N)$  where  $N$  is the number of states accessible by the neighborhood and the  $u_i$  are single qubit operations. We thus consider the update rules as multiply-controlled unitaries with target  $x$ . This feature will be key for considering the topology of the QCA at a given time.

#### 3.1 Block-Partitioned QCA

Given an infinite register  $\mathcal{R}$ , it is unclear as to how one defines appropriate local updates while ensuring unitarity of the global system.<sup>17,18</sup> A clear way avoid this is to implement partitioned QCA.

**DEFINITION 4.** *A partitioned QCA is a 6-tuple  $\{\mathcal{R}, S, \mathbf{B}, \Sigma, T, \mathcal{U}\}$  where  $\mathcal{R} = \mathbb{Z}^d$  is the register,  $S$  is a sublattice of  $\mathcal{R}$ ,  $\mathbf{B}$  is a partitioning scheme on  $\mathcal{R}$ ,  $\Sigma$  is a finite set of cell states,  $T$  is the local period for a global update, and  $\mathcal{U}$  is the local update rule.*

An example of a partitioned QCA is the block partitioned QCA (BPQCA).<sup>19</sup> On the register of sites, the qubits, the partitioning of the register is done according to species of qudits and the assignment of a neighborhood to each species. If one takes two species  $A$  and  $B$  and a nearest neighbor neighborhood, then a global update rule can be defined as the successive application of an update rule on the species  $B$  qudits (with their neighborhood) followed by the update on species  $A$  qudits.

To further simplify the computation (and more accurately model physical implementations), we will supplement the block-partitioning with boundary conditions. In a finite  $d$ -dimensional BPQCA, the register is given by  $\mathcal{R} = \mathbb{Z}_N^d$  with static boundaries given by ancillae qudits. The neighborhoods of sites near the boundary can then be reduced to just those sites within  $\mathcal{R}$ . In the rest of this manuscript, we will exclusively examine the geometry of such a block-partitioned QCA with sites containing qubits.

#### 3.2 1D QCA

Suppose now that  $\mathcal{R} = \mathbb{Z}_N$  and each site is a two-level system, i.e a qubit. We have a 1-dimensional BPQCA of  $N$ -qubits with two boundary qubits on the two ends of  $\mathcal{R}$ . We define the neighborhood of a site  $i$  as the set of nearest neighbors,  $\mathcal{N}_i = \{i-1, i+1\}$ . We block partition  $\mathcal{R}$  into two species, even (A) and odd (B) following Brennen, *et. al.*<sup>19</sup> The update rules are given by four unitary operators  $u_0, u_1, u_2, u_3 \in \text{SU}(2)$ . The subscript on these single-qubit operations labels the basis vectors for the Hilbert space of the qubits neighboring the site being updated, i.e.  $0 \rightarrow |00\rangle$ ,  $1 \rightarrow |01\rangle$ ,  $2 \rightarrow |10\rangle$ ,  $3 \rightarrow |11\rangle$ . The global update is the combined update  $U = U^A(u_0, u_1, u_2, u_3)U^B(u_0, u_1, u_2, u_3)$ . The update rule simplifies to  $U^0(u_0, u_1)$  and  $U^{(N-1)}(u_0, u_2)$  on the sites at the boundary of  $\mathcal{R}$ .

What is the topology generated by the evolution of this system? How does one measure the geometry? Let us examine first the update rule. Since the global update is decomposed into two distinct operations on  $\mathcal{R}$ , we examine each update as an individual time-step of the system. Following the arguments of Sections 2.2 and 2.3, we generate simplicial complexes based on the causal future of the slice in the computation. In the causal past of single local update, we have the local neighborhood  $\mathcal{N} \cup \{i\}$ . In general, this will be mapped to a 2-simplex.

The simplicial complex of the first non-trivial thickened anti-chain then becomes a chain of 2-simplexes with the edge  $\overline{i, i+1}$  shared by two such 2-simplexes. Any edge  $\overline{i, i+2}$  is contained in only one 2-simplex. As we increase the thickness and derive the simplicial complex on the initial slice, the effect is to add two-dimensions to the individual building blocks while retaining the global 1-dimensional nature, i.e. the system acts as a cylinder with a  $2t$ -dimensional cross-section. The infinite QCA is effectively 1-dimensional with local structure generated by interaction via the light cones.

If we utilize the fact that each local update rule  $U^i$  acts on  $\mathcal{N} \cup \{i\}$  as a multiply-controlled quantum gate, then we simplify the model and preserve the connected nature of the 1d BPQCA. We note that the controlled nature of the update rule is such that after a single update is applied, two sites,  $i$  and  $i+2$  have no causal influence on one another. They act simply as controls for site  $i+1$ . Hence, in modeling the causal behavior of the site, the simplicial complex incorporating the controlled-nature of the update removes the edges  $\overline{i, i+2}$ . The simplicial complex induced by a single update yields the topology of a discrete line. Increasing the thickness of the thickened anti-chain induces a topology on the slice that increases the dimensionality of the cross-sectional surfaces along the longitudinal axis, creating a cylinder of cross-sectional dimension  $d > 0$  (Figure 4). The topology is thus stable with a topology that is analogous to that of  $\mathbb{R}$ . It is consistent to take as the simplicial complex, the initial complex which is simply connected.

This construction yields a topology endowed with a local metric that has at most one local degree of freedom. The intrinsic geometry has no curvature and is entirely characterized by the local scale factor. We therefore specify the entire intrinsic geometry by giving the local distance between any two points in the topology. In the 1D BPQCA, this intrinsic geometry measures only bipartite correlations between nearest neighbors and carries no information about more distributed measures of farther separated correlations.

In some standard simulations of 1D BPQCA,<sup>19</sup> we demonstrate (Figure 5) propagation of an unknown qubit across the chain or generation of a GHZ state. We then generate distance information from the Zurek distance on the intrinsic geometry of the QCA. The register for the computation is the set of qubits  $\mathcal{Q} = \{q_1, \dots, q_N\}$  with boundary qubits  $\mathcal{B} = \{q_0, q_{N+1}\}$ . These qubits are partitioned into even (B) and odd (A) species. The single species update rule is given by  $U^{A(B)} := U^{A(B)}(\mathbb{1}, e^{-i\frac{\pi}{2}\sigma_x}, e^{-i\frac{\pi}{2}\sigma_x}, e^{-i\pi\sigma_x})$ . Propagation of an unknown state  $|q_1\rangle = |\psi\rangle$  is achieved by  $N/2$  successive applications of  $U = U^A U^B$  and a final  $Z$ -rotation on  $1_N$ . In Figure 5(a, c) we show results from the simulation on a 12 qubit register. It is interesting to note that if the update rule is applied to the seed  $|\mathcal{Q}\rangle = |100\dots 0\rangle$ , then no entanglement is generated. With an update rule and an initial seed in the same basis, the state stays separable and the information distance is 0 throughout the computation, i.e. the geometry of the computation is a point.

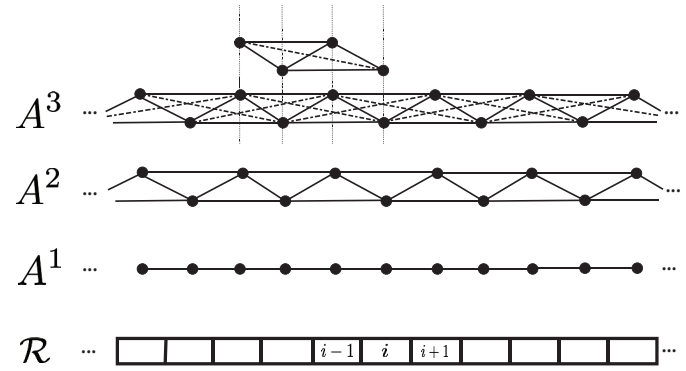


Figure 4. The simplicial complexes generated on a 1D BPQCA generated by thickened anti-chains. The thickness of the anti-chain corresponds to the number of local update rules applied, where  $A$  and  $B$  species updates are distinct. We see that as we increase the thickened anti-chain generating the complex, the global topology remains essentially constant, however, locally the system generates higher-dimensional cross-sections. Since there is no significant change in the topology as thickness increases, we can take the earliest simplicial complex in the stable regime of the filtered homology,  $A_1$ . This will represent the structure identifying neighboring qubits and determine how we specify information distances.



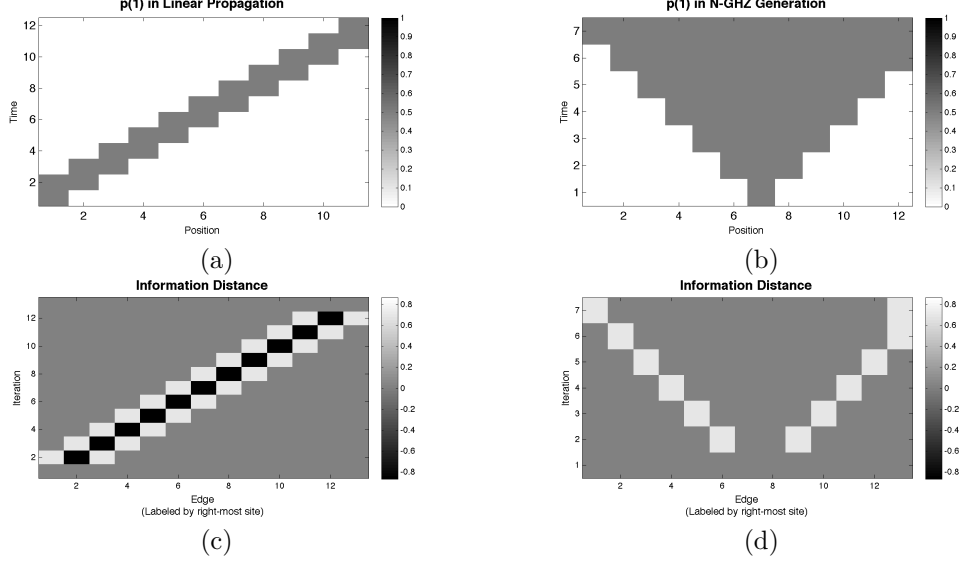


Figure 5. (a) The probability,  $p(1)$ , that the qubit is in the state  $|1\rangle$  for the propagation of a single qubit across the 12 qubit QCA. The color scale is such that black corresponds to 1 and white corresponds to 0. (b) The probability,  $p(1)$ , for generation of the 12-qubit GHZ state. (c) Information distances in the linear propagation of a qubit across the 1D BPQCA. We explicitly show the distances between qubits in the QCA and the fixed boundary qubits in this plot. Negative distances (black) correspond to bipartite entanglement, while white/light grey corresponds to positive information distances. (d) Information distances in GHZ generation. We see no evidence no bipartite quantum (negative distance) correlations. However, positive information distances form a boundary around the GHZ state. This positive distance boundary is key to identifying the form of entanglement present in the system.

To generate an  $N$ -GHZ state,

$$|N\text{-GHZ}\rangle = \frac{1}{\sqrt{2}} (|\underbrace{00\cdots 0}_{N\text{-times}}\rangle + |\underbrace{11\cdots 1}_{N\text{-times}}\rangle),$$

we follow the procedure above and seed  $q_{N/2}$  ( $q_{N/2+1}$ ) with  $|+\rangle$  when  $N \bmod 4 = 0$  ( $N \bmod 4 = 2$ ). The local, single-step update rule is again given by  $U^{A(B)} := U^{A(B)}(\mathbb{1}, e^{-i\frac{\pi}{2}\sigma_x}, e^{-i\frac{\pi}{2}\sigma_x}, e^{-i\pi\sigma_x})$  and is applied over  $k = N/4$  ( $k = (N - 2)/4$ ) iterations on both the  $A$  and  $B$  species, i.e.  $k$  global iterations or  $2k$  single-step iterations. When  $N \bmod 4 = 2$ , one must apply an additional single-step update on the  $B$  species. The final  $N$ -GHZ state is obtained after a single-qubit phase correction,  $e^{(-1)^k i\frac{\pi}{4}\sigma_z}$ . If we examine the geometry generated from this evolution, we find that any given slice yields no specific revelation as to the entanglement in the system. However, coupling together the intrinsic geometry of the slice with either the extrinsic geometric information (non-nearest neighbor information distances) or knowledge of the evolution of the system tells gives indications as to the structure of entanglement found in the system.

From the non-nearest neighbor distances we obtain a distance matrix of the form

$$\begin{pmatrix} 0 & 0 & 0 & d_{1i_1} & \cdots & d_{1i_n} & 0 & 0 & 0 \\ 0 & 0 & 0 & \vdots & \ddots & \vdots & 0 & 0 & 0 \\ 0 & 0 & 0 & d_{(i_1-1)i_1} & \cdots & d_{(i_1-1)i_n} & 0 & 0 & 0 \\ d_{i_1 1} & \cdots & d_{i_1(i_1-1)} & 0 & \cdots & 0 & d_{i_1(i_n+1)} & \cdots & d_{i_1 N} \\ \vdots & \ddots & \vdots & \vdots & \ddots & \vdots & \vdots & \ddots & \vdots \\ d_{i_n 1} & \cdots & d_{i_n(i_1-1)} & 0 & \cdots & 0 & d_{i_n(i_n+1)} & \cdots & d_{i_n N} \\ 0 & 0 & 0 & d_{(i_n+1)i_1} & \cdots & d_{(i_n+1)i_n} & 0 & 0 & 0 \\ 0 & 0 & 0 & \vdots & \ddots & \vdots & 0 & 0 & 0 \\ 0 & 0 & 0 & d_{Ni_1} & \cdots & d_{Ni_n} & 0 & 0 & 0 \end{pmatrix} \quad (7)$$

where  $d_{ij} > 0$  and the string of qubits  $\{q_{i_1}, \dots, q_{i_n}\}$  is dependent on the global iteration number of the QCA. Since the global state is pure, the existence of non-zero distances indicates non-local correlations in the system. The structure of the distance matrix demonstrates multipartite entanglement on the qubits in a block whose information distances are all null. This is clear since the distance between any qubit in the interior block and any qubit outside the block is positive, the distances inside the block are all null, and the distances between qubits entirely outside the block are all 0. We need only identify whether the interior block or exterior block contains multipartite, non-local correlations. Since on the first iteration,  $q_1$  cannot have causal influence or be causally influenced by qubits outside its neighborhood, we must find that the interior block exhibits non-local correlations. Extending this from iteration 1 to iteration  $k$  allows us to determine the location of multi-partite non-local correlations at any instance in the QCA for this example.

If we instead wish to keep the focus on the intrinsic geometry and the causal evolution, we again can make certain observations about the nature of non-local correlations in the system. We recognize that causal influence has a finite velocity in the system and that the system starts in a separable state. The state at any iteration  $j \geq 1$  has the general property that there are three regions within which the information distances are all null. We can simplify this to two regions, the exterior and interior in an obvious way. We assume we know only the information distances and not necessarily the state of the system at any iteration. As we iterate, we have two options: (1) The two regions separated by the positive distance boundary are regions of separable states (with possible non-local correlations between them), or (2) one of the regions is a set of qubits exhibiting multipartite non-local correlations. We can rule out the first immediately as the global system is pure and at the first iteration non-local correlations between the two subsets of qubits would be impossible given the update rule. On the latter option, any region containing  $q_1$  would then require non-local correlations between  $q_1$  and a qubit outside its local neighborhood. As before, this is a scenario that is impossible given the finite velocity of causal influence in the QCA. Applying this to either of the exterior regions and following the evolution tells us that there must be multipartite, non-local correlations on the set  $\{q_{i_1}, \dots, q_{i_n}\}$ .

We now consider an example where the bipartite entanglement is not so straightforward. We take as the single-step update rule  $U^{A(B)}(\mathbb{1}, e^{-i\frac{\pi}{3}\sigma_x}, e^{-i\frac{\pi}{3}\sigma_x}, e^{-i\pi\sigma_x})$ . The register is seeded with  $|q_i\rangle = |+\rangle$  and all other  $|q_j\rangle = |0\rangle$  ( $j \neq i$ ). In this case, the update rule generates some entanglement between pairs, and distributes the entanglement as the computation goes forth. Figure 6 shows both the reduced entropy and the information distance for this update rule. Non-zero reduced entropy of a qubit  $q_k$  in a system where the global state is pure (and hence has zero entropy) can indicate the presence of entanglement between the reduced system and the state of  $\mathcal{Q} - q_k$ . However, the nature of the entanglement is not clear. Instead, the information distance in the intrinsic geometry gives us the ability to identify the existence of local (nearest neighbor), bipartite entanglement. The negative information distances correspond to the necessary presence of quantum, non-local correlations, and the positive distances still provide a measure of the existence of entanglement between a qubit and some distant subset of the QCA not immediately connected to it.

From the local nature of the simplicial complex, we see that the information distance as a measure of the intrinsic geometry can only tell us about the correlations between nearest neighbors. In cases where the information distance is negative, we have direct indication of quantum, non-local correlations. We have already discussed how to utilize either the extrinsic geometry or causal content to identify multipartite non-local correlations that still may lead to non-negative distances. However, this was specific to generation of the GHZ state. In more general cases, we could relax the assumption of taking the earliest simplicial complex in the stable regime of the filtered (with respect to the thickened anti-chains) homology. We could instead use the simplicial complexes with thickened anti-chains built into the past of the anti-chain  $A_j$ . It would be natural then to take the thickness equal to the number of iterations performed. This would amount to an accumulation of the past light cone into a mutually interacting simplex in the cross section of the topological cylinder,  $S^d \times \mathbb{R}$ . An alternative is to couple the intrinsic geometry with an embedding in the space constructed from information distances between all bipartite decompositions of all possible subsets in the system. This is not favorable as the parameters in this type of model scales exponentially with the number of qubits.

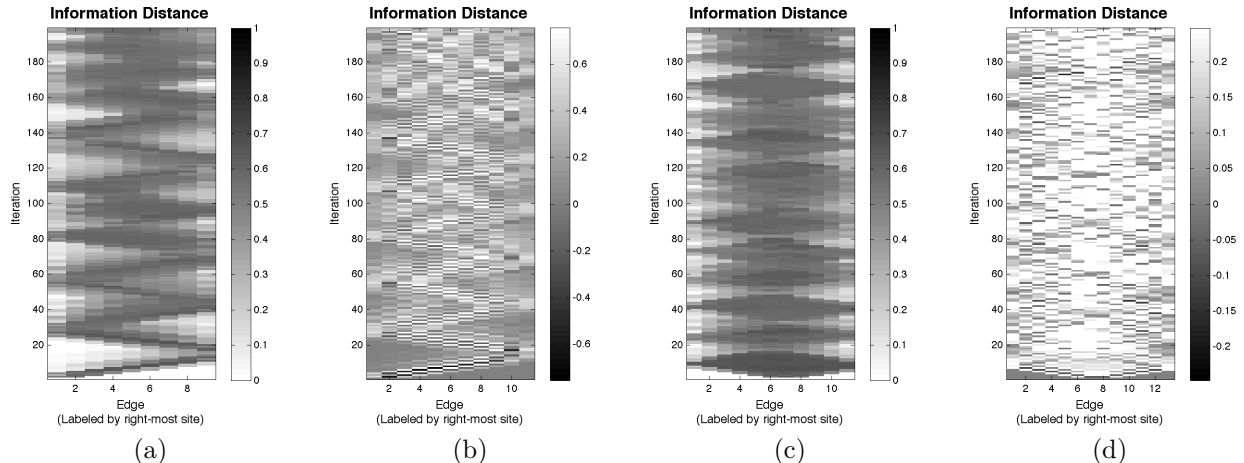


Figure 6. The QCA with update rule  $U^{A(B)}(\mathbb{1}, e^{-i\frac{\pi}{3}\sigma_x}, e^{-i\frac{\pi}{3}\sigma_x}, e^{-i\pi\sigma_x})$ . (a) The reduced entropy,  $S(q_i)$ , obtained through partial trace over  $\mathcal{Q}-q_i$ . The QCA of 10 qubits is seeded with qubit  $|q_1\rangle = |+\rangle$ . We see that  $S(q_i)$  is always positive on the sites. (b) The information geometry shows distinct regions of bipartite entanglement. Bipartite entanglement is captured by negative information distances (darker regions) in the geometry. Lighter regions correspond to the positive information distances in which classical correlations are most prevalent. While it is possible to identify entanglement via negative information distances, positive distances in the geometry do not necessarily correspond to lack of entanglement. (c) The reduced entropy on the QCA with 12 qubits seeded with qubit  $|q_{\frac{N}{2}+1}\rangle = |+\rangle$ . (d) The information distances on the same system as (c). Again local, bipartite quantum correlations propagate and diffuse as the QCA progresses. However, we can identify instances in the computation where nearest neighbors exhibit such quantum correlations. Extending information distances to geometric content beyond the intrinsic topology can lead to richer characterization of the geometry and entanglement.

#### 4. DISCUSSION

We have proposed here a new view of quantum computation based on the configuration of qubits at any given time of the computation. Central to this proposed perspective is that one of the essential features of the computation is not the exact states of the qubits in the computation, but rather the information content in the configuration of qubits. A pure, separable state of  $N$ -qubits contains no more information than if the qubits are set in the computational state  $|00\cdots 0\rangle$ , since local unitaries applied to the individual qubits that rotate each qubit into the zero state do not change the information content. Indeed, there is no physical distinction between an arbitrary, pure, separable state and the state  $|00\cdots 0\rangle$ , only a local basis change. We see this in the information distance as the total absence of any geometric content in such a state. The ability of a computation to yield a given output is contained in the correlations in the constituents of the geometry. To give the particular state of the computation is akin to coordinatizing the geometry. This situation can be likened to that of general relativity in which one is perfectly allowed to ask the position or state of a particle/system with respect to some coordinates or even some other reference system. However, in general relativity it is not reasonable to ask of the physical system the *absolute* position or momentum of a particle/system. Likewise, in quantum computation when we put a set qubits into the computational basis, we have specified a coordinatization on the states. This coordinatization does not carry in it any physical content.

This is not a view that is incompatible from the view proposed by Nielsen, *et. al.*<sup>1,2</sup> where the emphasis was on the unitary operators in the computation. There, one need not specify an initial or final state as it is not necessarily relevant to the computation. Rather, the relevant content is contained in how the information is distributed across the qubits and how the system has changed from the initial to the final states.

In a quantum system one may only ask questions with respect to a certain type of measurement.<sup>20</sup> Without such specification, it is impossible to make heads or tails of the qubits in the computation. We only extract information from the computation by composing a string of bits based on the yes/no questions with respect to a given basis for each qubit. Without such coordinatization, the state of the string of qubits has given no direct

answer. The ability to extract the result of computation is only realized when we know what questions to ask, i.e. when we know with respect to which coordinization the system is to be evaluated. Of course, even then, the system will not have a unique state from which to extract the answer. The result of the quantum computation is the *in toto* information encoded in the qubits, independent of local unitary transformations. This is similar to the situation one must face in general relativity where the physical content is encoded in quantities invariant under local  $GL(4)$  transformations that can modify the local basis, the metric components, *etc.*

This present manuscript has outlined this approach and provided some initial analysis on 1D QCA. The analysis of non-local correlations in QCA shows some functional possibilities of generating the computational geometry. Foremost is the ability to identify bi-partite entanglement. We have shown explicitly the appearance of negative information distances as a way to identify quantum correlations. However, negative distances are only sufficient and not necessary for there to be quantum correlations present in a general mixed state. A complete classification of entanglement in a quantum computation (on pure states) requires either a deeper analysis on the decomposition of information distance into classical and quantum components and/or the distance measures between all possible bipartite pairs in the quantum system. For classification of entanglement in computations on mixed states, it is necessary to examine the decomposition of the information distance into classical and quantum components along the lines of Vedral, *et. al.*<sup>8</sup>

The application of this approach to 1D QCA shows some utility in identifying topologically local quantum correlations. As we extend this approach to higher-dimensional cases, the geometric content of the distance information imposed on the topological scaffolding becomes much more rich. Beyond information distance, it will be necessary to understand quantities such as information areas or volumes. The intrinsic topology of the computation at any given time was constructed so as to identify paths of information flow as the computation moves forward. Higher dimensional analogs of this notion will aim to indicate the correlations between many qubits who share mutual influence. Higher dimensional examples will additionally allow us to incorporate curvature as way to study the information flow through the system. Recent work in information flow on networks has suggested that the curvature gives an indication of the load-balancing or congested nature of the information flow.<sup>21</sup>

With the notion that curvature gives indication as to load-balancing or congestion in an information carrying/processing system, one way to optimize a quantum computation is to distribute the computation across the quantum register. Optimally distributing the information processing will ensure maximum use of quantum parallelism, i.e. maximal utilization of the degrees of freedom available to the register. Such optimization can, in principle, be achieved by applying geometric gradient flows, e.g. Ricci flow,<sup>22</sup> act as diffusive flows for curvature. Future work will focus on extending this current approach to higher-dimensional models that allow for such an analysis on the curvature in the computation.

## ACKNOWLEDGMENTS

JRM was supported through a National Research Council Research Associateship Award at AFRL Information Directorate for this research. PMA and JRM acknowledge the partial support of the Air Force Office of Scientific Research (AFOSR) for this work. HAB acknowledges support from AFRL Information Directorate under grant FA 8750-11-2-0275. JRM, PMA, and HAB would like to thank Warner A. Miller for numerous helpful discussions. Any opinions, findings, and conclusions or recommendations expressed in this material are those of the authors and do not necessarily reflect the views of AFRL.

## REFERENCES

- [1] Nielsen, M. A., Dowling, M. R., Gu, M., and Doherty, A. C., “Quantum computation as geometry,” *Science* **311**(5764), 1133–1135 (2006).
- [2] Gu, M., Doherty, A., and Nielsen, M. A., “Quantum control via geometry: An explicit example,” *Phys. Rev. A* **78**, 032327 (2008).
- [3] Blute, R. F., Ivanov, I. T., and Panangaden, P., “Discrete Quantum Causal Dynamics,” *Int. J. Theor. Phys.* **42**(9), 2025–2041 (2003).

- [4] Zurek, W. H., “Thermodynamic cost of computation, algorithmic complexity and the information metric,” *Nature* **341**(6238), 119–124 (1989).
- [5] Schumacher, B., “Information and quantum nonseparability,” *Phys. Rev. A* **44**(11), 7047–7052 (1991).
- [6] Feynman, R. P., “Simulating physics with computers,” *Int. J. Theor. Phys.* **21**(6/7), 467–488 (1982). reprinted in [*Feynman and Computation*], A.J.G. Hey (ed.), Perseus Books: Reading, MA (1999).
- [7] Olliver, H. and Zurek, W., “Quantum Discord: A Measure of the Quantumness of Correlations,” *Phys. Rev. Lett.* **88**(1), 017901 ( 4 pp) (2002).
- [8] Vedral, V., Plenio, M. B., Rippin, M. A., and Knight, P. L., “Quantifying entanglement,” *Phys. Rev. Lett.* **78**, 2275–2279 (1997).
- [9] Kronheimer, E. and Penrose, R., “On the structure of causal spaces,” *Proc. Cambridge Phil. Soc.* **63**, 481–501 (1967).
- [10] Major, S., Rideout, D., and Surya, S., “On recovering continuum topology from a causal set,” *J. Math. Phys.* **48**(3), 2501 (2007).
- [11] Kaczynski, T., Mischaikow, K., and Mrozek, M., [*Computational Homology (Applied Mathematical Sciences)*], Springer, 1 ed. (Jan. 2004).
- [12] Zomorodian, A., “Computational Topology,” *Algorithms and Theory of Computation Handbook* , 395 (2009).
- [13] Carlsson, G., “Topology and data,” *Bull. Amer. Math. Soc.(NS)* **46**(2), 255–308 (2009).
- [14] Aleksandrov, P., [*Combinatorial Topology*], vol. 1, Graylock Press, Baltimore (1956). translation by H. Komm.
- [15] Grössing, G. and Zeilinger, A., “Quantum cellular automata,” *Complex Systems* **2**(2) (1988).
- [16] Watrous, J., “On one-dimensional quantum cellular automata,” *Proc. of the 36th Annual Symposium on Foundations of Computer Science* , 528–537 (1995).
- [17] Schumacher, B. and Werner, R. F., “Reversible quantum cellular automata,” *arXiv.org quant-ph*, 5174 (2004).
- [18] Perez-Delgado, C. A. and Cheung, D., “Local unitary quantum cellular automata,” *Phys. Rev. A* **76**(3), 32320 (2007).
- [19] Brennen, G. and Williams, J., “Entanglement dynamics in one-dimensional quantum cellular automata,” *Phys. Rev. A* **68**(4) (2003).
- [20] Wheeler, J., “How Come the Quantum?,” *Annals of the New York Academy of Sciences* **480**(1), 304–316 (1986).
- [21] Jonckheere, E. and Lohsoonthorn, P., “Geometry of network security,” *Proc. of the 2004 American Control Conference* **2**, 976–981 (2004).
- [22] Hamilton, R., “Three-manifolds with positive Ricci curvature,” *J. Differential Geom* **17**(2), 255–306 (1982).